

OPEN

Plasmodium Infection Induces Dyslipidemia and a Hepatic Lipogenic State in the Host through the Inhibition of the AMPK-ACC Pathway

George Eduardo Gabriel Kluck¹, Camila Hübner Costabile Wendt², Guinever Eustaquio do Imperio³, Maria Fernanda Carvalho Araujo¹, Tainá Correa Atella⁴, Isabella da Rocha¹, Kildare Rocha Miranda³ & Georgia Correa Atella¹

Malaria is a major parasitic disease of humans and is a health public problem that affects more than 100 countries. In 2017, it caused nearly half a million deaths out of 219 million infections. Malaria is caused by the protozoan parasites of the genus *Plasmodium* and is transmitted by female mosquitoes of the genus *Anopheles*. Once in the bloodstream, *Plasmodium* merozoites invade erythrocytes and proliferate until the cells lyse and release new parasites that invade other erythrocytes. Remarkably, they can manipulate the vertebrate host's lipid metabolism pathways, since they cannot synthesize lipid classes that are essential for their development and replication. In this study, we show that mice infected with *Plasmodium chabaudi* present a completely different plasma profile from control mice, with marked hyperproteinemia, hypertriglyceridemia, hypoglycemia, and hypocholesterolemia. In addition, white adipose and hepatic tissue analyses from infected animals revealed the accumulation of triacylglycerol in both tissues and free fatty acids and free cholesterol in the liver. Hepatic mRNA and protein expression of key enzymes and transcription factors involved in lipid metabolism were also altered by *P. chabaudi* infection, leading to a lipogenic state. The enzyme 5' AMP-activated protein kinase (AMPK), a master regulator of cell energetic metabolism, was also modulated by the parasite, which reduced AMPK phosphorylation levels upon infection. Pretreatment with metformin for 21 days followed by infection with *P. chabaudi* was effective in preventing infection of mice and also lowered the hepatic accumulation of lipids while activating AMPK. Together, these results provide new and important information on the specific molecular mechanisms induced by the malaria parasite to regulate hepatic lipid metabolism in order to facilitate its development, proliferation, and lifespan in its vertebrate host.

Malaria is a major parasitic disease of humans¹. It is a life-threatening disease² and yet is considered to be a neglected disease and public health problem affecting more than 100 countries worldwide³. In 2017, it caused nearly half a million deaths out of 219 million infections. More than three billion people are at risk of being infected and developing malarial disease at this very moment⁴.

Malaria is an infectious disease caused by protozoan parasites of the genus *Plasmodium* and is transmitted by female mosquitoes of the genus *Anopheles*⁵. As a multifactorial disease, its clinical progression depends on several host factors, including age, previous exposure to infection, nutritional status, genetics of the host and

¹Laboratory of Lipid and Lipoproteins Biochemistry, Leopoldo de Meis Institute of Medical Biochemistry, Federal University of Rio de Janeiro, Rio de Janeiro, Brazil. ²Laboratory of Cellular Ultrastructure Hertha Meyer, Carlos Chagas Filho Institute of Biophysics, Federal University of Rio de Janeiro, Rio de Janeiro, Brazil. ³Laboratory of Translational Endocrinology, Carlos Chagas Filho Institute of Biophysics, Federal University of Rio de Janeiro, Rio de Janeiro, Brazil.

⁴Laboratory of Comparative Neurobiology and Development, Carlos Chagas Filho Institute of Biophysics, Federal University of Rio de Janeiro, Rio de Janeiro, Brazil. Correspondence and requests for materials should be addressed to G.C.A. (email: atella@bioqmed.ufrj.br)

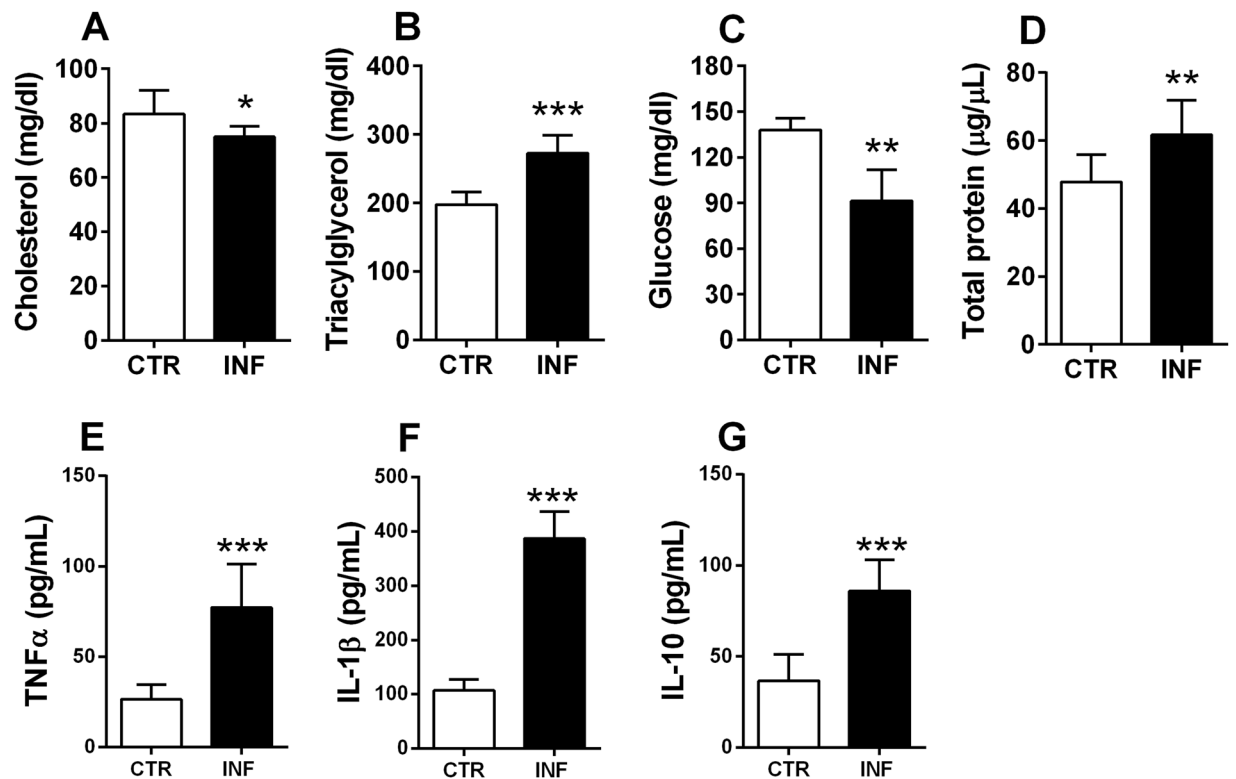


Figure 1. Plasma analysis of *P. chabaudi* infected mice. (A) Total cholesterol, (B) triacylglycerol, and (C) glucose concentrations obtained using enzymatic colorimetric assays. (D) Total protein concentration measured by the Lowry method. (E–G) TNF α , IL-1 β , and IL-10 concentration measured by ELISA. White bars indicate control (CTR, $n = 14$) and black bars indicate infected (INF, $n = 14$) groups. Statistical analyses: unpaired Student's *t*-test. Values are presented as mean \pm standard error. * $p < 0.05$, ** $p < 0.01$, and *** $p < 0.001$.

parasite, geographic location, and socioeconomic status^{6–8}. There are some events, however, that are fundamental to malarial pathogenesis: (1) the massive release of proinflammatory cytokines induced by the rupture of infected erythrocytes, (2) the adhesion of infected red blood cells (RBCs) in capillaries, and (3) the rupture and removal of infected RBCs by splenic macrophages. Together, these phenomena are responsible for the major syndromes associated with malaria, such as systemic inflammation, anemia, metabolic acidosis, and placental and cerebral malaria^{6–8}. In the liver, *Plasmodium* infection is associated with portal tract inflammation⁹, cholestasis⁹, RBCs sequestration, and hepatocytes necrosis¹⁰. Therefore, patients with malaria usually present with hepatomegaly, jaundice, an increased hepatic load of RBCs, and elevated serum levels of hepatic enzymes¹¹.

The liver is a central metabolic organ and is the main regulator of glucose and lipid metabolism, masterfully performing gluconeogenesis, β -oxidation, lipogenesis, and uptake and secretion of lipoproteins¹². The enzyme 5' AMP-activated protein kinase (AMPK) is a key regulator of liver lipid metabolism¹³. When activated, AMPK phosphorylates and inhibits the enzymes acetyl-CoA carboxylase (ACC) and 3-hydroxy-3-methylglutaryl-coenzyme A reductase (HMGCR), decreases fatty acid synthase (FAS) expression, and activates malonyl-CoA carboxylase, which leads to a reduction in fatty acid and cholesterol synthesis^{14–16}. The inhibition of ACC also stimulates fatty acids' oxidation through a decrease of malonyl-CoA^{17,18}, leading to an increased activity of carnitine palmitoyl transferase 1 (CPT1)¹⁹.

Considering that the metabolic consequences and the specific hepatic molecular mechanisms underlying the pathogenesis of malaria are still unclear, we aimed to investigate changes in lipid metabolism during *Plasmodium chabaudi* infection in mice in order to better understand their importance to the host–parasite interaction and to the outcome of the infection.

Results

P. chabaudi infection induces plasma dyslipidemia and altered profile of cytokines in swiss mice.

To evaluate the plasma profiles of infected mice, plasma samples were analyzed for total cholesterol, triacylglycerol (TAG), glucose, total protein, tumor necrosis factor alpha (TNF α), interleukin (IL)-1 β , and IL-10 concentrations (Fig. 1). Total cholesterol and glucose levels decreased significantly in infected mice compared to controls ($p < 0.05$ and $p < 0.01$, respectively; Fig. 1A,C), whereas TAG and total protein levels increased in infected animals ($p < 0.001$ and $p < 0.01$, respectively; Fig. 1B,D). TNF α , IL-1 β , and IL-10 concentrations increased significantly in infected mice compared to control group ($p < 0.0001$, $p < 0.0001$ and $p < 0.0001$, respectively; Fig. 1E–G). Together, these results revealed marked changes in plasma lipids, protein, and cytokines in infected versus control mice, suggesting dyslipidemia and inflammation response induced by infection.

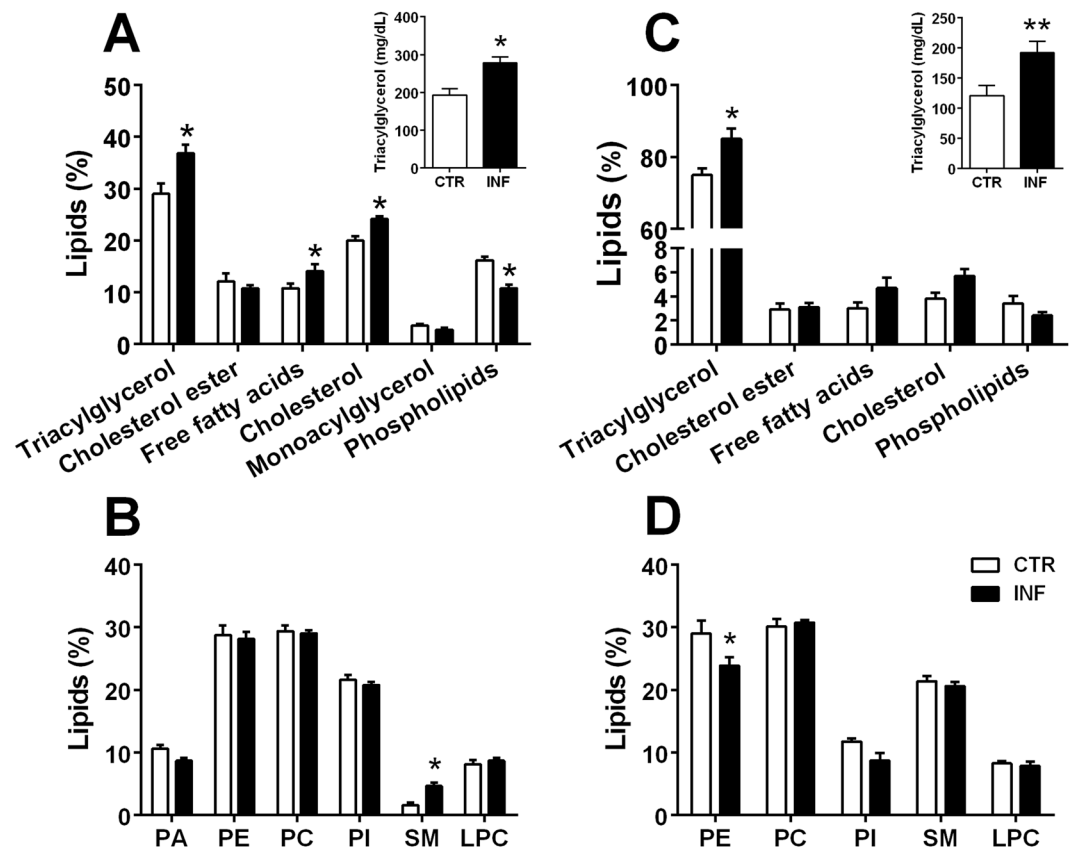


Figure 2. Lipid profile analysis in the liver (A,B) and white adipose tissue (WAT; C,D) of mice infected with *P. chabaudi*. The graphs show lipid classes obtained through thin-layer chromatography and percentages determined by densitometric analysis. Hepatic (A) and WAT (C) analyses of neutral lipids showing the percentage of triacylglycerol (TAG), cholesterol ester (CHOE), free fatty acid (FFA), cholesterol (CHO), monoacylglycerol (MAG), and phospholipid (PHO) in respective tissues of control (CTR, $n = 14$) versus infected (INF, $n = 14$) mice. Insets in (A,C) upper right represent TAG concentration obtained using enzymatic colorimetric assays. Hepatic (B) and WAT (D) analyses of phospholipids showing the percentage of phosphatidic acid (PA), phosphatidylethanolamine (PE), phosphatidylcholine (PC), phosphatidylinositol (PI), sphingomyelin (SM), and lysophosphatidylcholine (LPC) in respective tissues of CTR versus INF animals. Statistical analyses: multiple t -test. Values are presented as mean \pm standard error. * $p < 0.05$ and ** $p < 0.01$.

***P. chabaudi* promotes changes in lipid classes in the liver and white adipose tissue (WAT) of infected mice.** Analysis of hepatic and WAT lipid profiles was performed to investigate the possible alterations in lipid classes during *Plasmodium* infection. As shown in Fig. 2A,B, hepatic TAG ($p < 0.05$), free cholesterol ($p < 0.05$), free fatty acids ($p < 0.05$), and sphingomyelin (SM; $p < 0.05$) levels increased in infected animals relative to controls, whereas the WAT of infected animals exhibited elevated TAG ($p < 0.05$; Fig. 2C) and decreased phosphatidylethanolamine (PE; $p < 0.05$; Fig. 2D), with no significant differences found in the other lipid classes. Enzymatic colorimetric assays were used to confirm the hepatic and WAT changes in the TAG concentration and validate the increase of this lipid class in both tissues in the infected versus control groups (inset in Fig. 2A,C). Together, these data indicate that *P. chabaudi* infection induces an increase in lipid accumulation in tissues that are critical to lipid metabolism in mice.

***P. chabaudi* infection leads to an altered hepatic expression of genes associated with lipid metabolism.** After demonstrating that *Plasmodium* infection in mice induces a wide spectrum of lipid changes, including alterations in plasma lipids and hepatic and WAT lipid classes, we next hypothesized that *P. chabaudi* specifically impairs the gene expression of key enzymes and transcription factors involved in lipid degradation or biosynthesis (Table 1). In this respect, the transcription factors peroxisome proliferator-activated receptor- α (PPAR- α) and PPAR gamma coactivator-1 α (PGC-1 α) and the β -oxidation enzyme CPT1-A were chosen for investigation as genes involved in lipid degradation pathways; all decreased significantly in infected mice ($p < 0.001$; Fig. 3A–C). The transcription factor PPAR- γ and the enzymes FAS and ACC were chosen to assess the mediators of lipid biosynthesis pathways; PPAR- γ and FAS levels increased in infected mice ($p < 0.05$ and $p < 0.01$; Fig. 3D,E), with no significant difference in the ACC gene expression (Fig. 3F). Together, these findings demonstrate that malaria induces significant changes in hepatic gene expression, whose combination points to an increase in lipogenic and a decrease in lipolytic pathways.

Primer	Forward	Reverse
<i>Acaca</i>	5'-AACATCCCCACGCTAACAG-3'	5'-CTGACAAGGTGGCGTGAAG-3'
<i>Cpt1a</i>	5'-AGTGGCCTCACAGACTCCAG-3'	5'-CCCATGTTGTACAGCTTCC-3'
<i>Fasn</i>	5'-CCCTTGATGAAGAGGGATCA-3'	5'-GAACAAGCGTTAGGGTTGA-3'
<i>Ppargc1a</i>	5'-ATGTGTCGCCTTCTTGCTCT-3'	5'-ATCTACTGCCTGGGGACCTT-3'
<i>Ppara</i>	5'-CAGTGGGGAGAGAGGACAGA-3'	5'-AGTTCGGGAACAAGACGTTG-3'
<i>Pparg</i>	5'-GATGGAAGACACTCGCATT-3'	5'-AACCATTGGGTGAGCTCTTG-3'

Table 1. Primers sequence used for gene expression assessment. *Acaca*: acetyl-coa carboxylase; *Cpt1a*: carnitine palmitoyl transferase; *Fasn*: fatty acid synthase; *Ppargc1a*: peroxisome proliferator-activated receptor gamma coactivator 1-alpha; *Ppara*: peroxisome proliferator activated receptor alpha; *Pparg*: peroxisome proliferator activated receptor gamma.

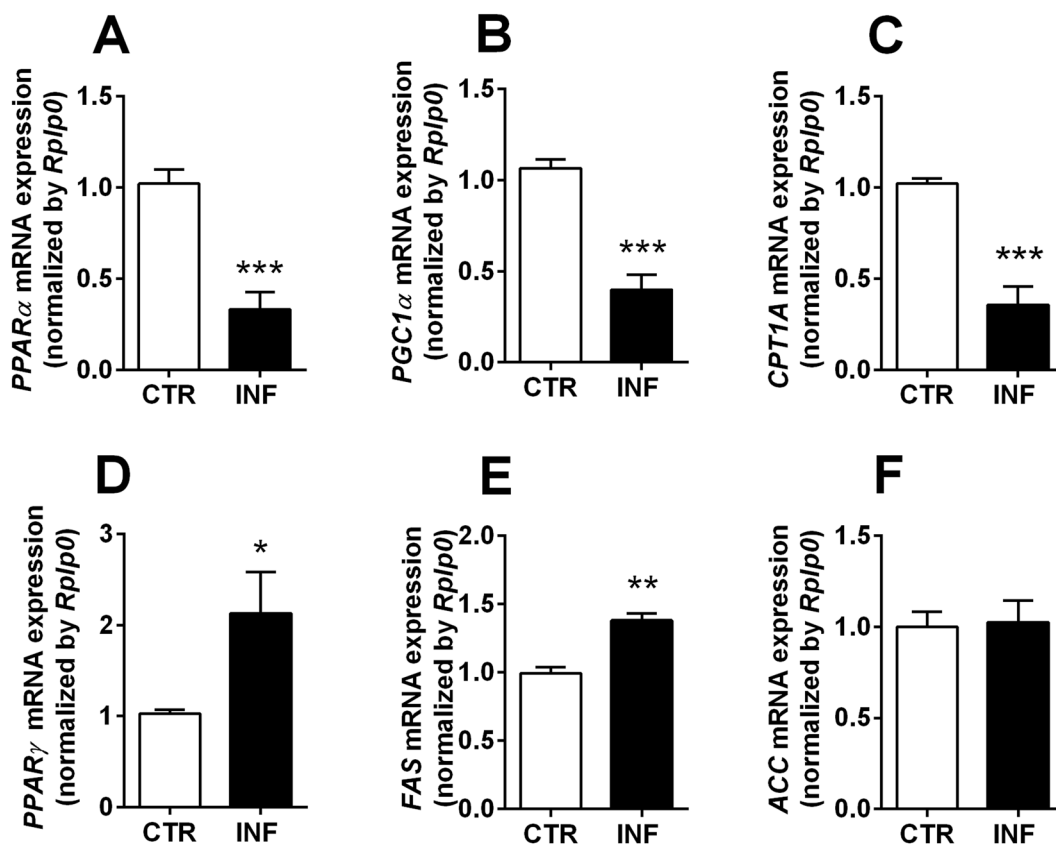


Figure 3. Gene expression of key enzymes and transcription factors involved in lipid metabolism in the liver of mice infected with *P. chabaudi*. PPAR- α (A), PGC-1 α (B), CPT1-A (C), PPAR- γ (D), FAS (E), and ACC (F) gene expression analysis. *Rplp0* was used as an endogenous control. White bars indicate control (CTR, $n = 14$) and black bars indicate infected (INF, $n = 14$) groups. Statistical analyses: unpaired Student's *t*-test. Values are presented as mean \pm standard error. * $p < 0.05$, ** $p < 0.01$, and *** $p < 0.001$.

***P. chabaudi* infection modifies the phosphorylation levels and protein expression of hepatic enzymes and transcription factors involved in lipid metabolism.** AMPK is a master regulator of cellular energetic metabolism²⁰. When phosphorylated, this kinase is activated and also uses phosphorylation to downregulate anabolic and stimulate catabolic pathways in order to restore cellular energy balance²⁰. Thus, we hypothesized that hepatic phosphorylation levels of AMPK and its downstream targets would be altered by *P. chabaudi* infection in these animals. We then demonstrated that AMPK phosphorylation levels decrease significantly upon infection ($p < 0.05$; Fig. 4A and Supplementary S1A), which is accompanied by decreased phosphorylation of ACC, the transcription factor sterol regulatory element binding protein-1c (SREBP-1c), and PPAR α ($p < 0.001$; Fig. 4B,C,E, respectively and Supplementary S1B,C,F). Also, there was an increased protein expression of FAS and PPAR γ ($p < 0.05$; Fig. 4D,E; Supplementary S1D,E).

Pretreatment with metformin reduces *P. chabaudi* infection in mice and protects the liver against steatosis. In order to validate the critical role of AMPK-mediated lipid metabolism alteration induced

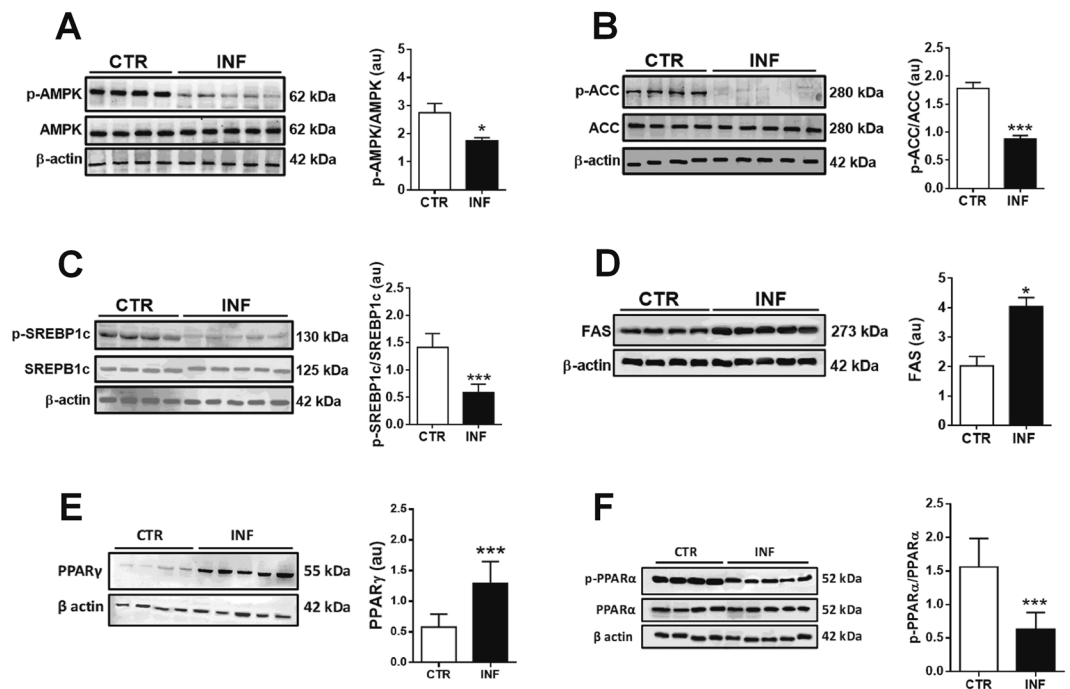


Figure 4. Protein expression of key enzymes and transcription factors involved in lipid metabolism in the liver of mice infected with *P. chabaudi*. Representative immunoblots and the quantification of phosphoprotein (p) and/or total protein levels of AMPK (A), ACC (B), SREBP-1c (C), FAS (D), PPAR α (E), and PPAR γ (F). β -Actin was used as loading controls. Images represents cropped blots of the same membrane. Cropped slices are showed on Supplementary Information (S1). White bars indicate control (CTR, $n = 14$) and black bars indicate infected (INF, $n = 14$) groups. Statistical analyses: unpaired Student's *t*-test. Values are presented as mean \pm standard error. * $p < 0.05$ and *** $p < 0.001$.

by infection, mice were pretreated with the AMPK activator metformin (1,1-dimethyl biguanide) prior to *P. chabaudi* inoculation (see Materials and Methods). Metformin pretreatment completely reversed the decrease in hepatic AMPK phosphorylation levels observed following *P. chabaudi* infection ($p < 0.001$; Fig. 5A and Supplementary S2A). Similarly, metformin pretreatment abolished the decrease and even increased the hepatic phosphorylation of ACC (a downstream target of AMPK) in the infected metformin group compared to the infected ($p < 0.001$) and control ($p < 0.001$; Fig. 5B and Supplementary S2B) groups. Remarkably, while infected mice presented a gradual and marked increase in parasitemia percentage, reaching 80% on the 5th day after infection (Fig. 6), pretreatment with metformin resulted in a dramatic reduction of the parasitemia percentage from the 3rd to the 5th day after infection ($p < 0.001$; Fig. 6). This significant drop in the infection rate was also accompanied by reduced clinical signs of infection, such as lethargy, piloerection, hypothermia, starvation, and anemia were all abrogated in the pretreated infected animals compared to the untreated infected mice. In addition, pretreatment with metformin induced a decrease in the percentage of all hepatic lipid classes both in infected and in noninfected mice ($p < 0.001$; Fig. 7), except for total phospholipids, which were higher than in the nontreated groups ($p < 0.001$; Fig. 7). Pretreatment with metformin caused a significantly decrease on TNF α , IL-1 β and IL-10 both in plasma and liver of infected mice compared to control group (Fig. 8A–F).

Discussion

In this study, we demonstrated that *P. chabaudi* infection induces severe changes in the vertebrate host's lipid metabolism that manifest as plasma, hepatic, and WAT metabolic modifications. These changes are mediated by AMPK downregulation and the subsequent activation of pathways that lead to increased lipid biosynthesis and accumulation. Pretreatment with metformin reversed hepatic changes induced by infection, suggesting the establishment of a protective metabolic state that inhibited pathogen proliferation and consequently dissemination in the mammal host.

The balance between host pro- and anti-inflammatory immune responses plays a critical role in determining the outcome of *Plasmodium* infection. A weak pro-inflammatory response may result in unregulated replication of parasites, while an active pro-inflammatory response may cause tissue damage, such as occurs in severe malaria syndromes, including cerebral malaria and multi-organ failure. Here, we showed an increased TNF α , IL-1 β , and IL-10 in plasma and liver of infected mice compared to control group (Fig. 1). High levels of plasma TNF α have been associated with anemia and high density *P. falciparum* infection²¹, as well as with other severe malaria complications such as renal failure²². Data from mouse models of malaria indicates that IL-10 is required to protect host tissue from inflammation, but may also promote growth of parasites and associated disease manifestations.

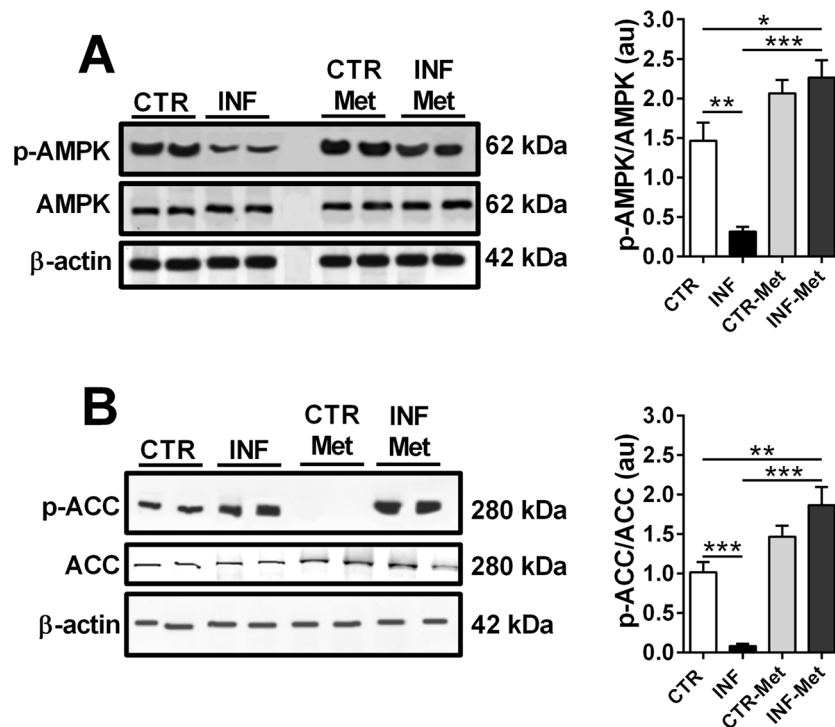


Figure 5. Effect of metformin pretreatment on the protein expression of AMPK and ACC in the liver of mice infected with *P. chabaudi*. Representative immunoblots and quantification of phosphorylation levels of AMPK (A) and ACC (B). Images represent cropped blots of the same membrane. Cropped slices are shown on Supplementary Information (S2). White bars indicating control (CTR, $n = 9$), black bars indicate infected (INF, $n = 9$), light gray bars indicate metformin pretreated control (CTR-Met, $n = 9$), and dark gray bars indicate metformin pretreated infected (INF-Met, $n = 7$) groups. Statistical analyses: one-way ANOVA followed by Dunnett's multiple comparisons test. Values are presented as mean \pm standard error. *** $p < 0.001$.

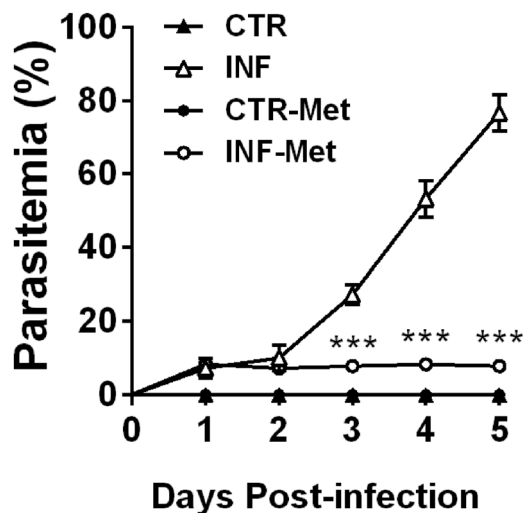


Figure 6. Effect of metformin pretreatment on the effectiveness of *P. chabaudi* infection in mice. Percentage parasitemia assessed through evaluation of blood smears every day until the 5th day after infection. Closed triangles represent controls ($n = 9$), closed circles represent metformin pretreated controls ($n = 9$), open triangles represent the infected group ($n = 9$), and open circles represent the infected group pretreated with metformin ($n = 7$). Statistical analysis: two-way ANOVA followed by Tukey's multiple comparisons test. Values are presented as mean \pm standard error. *** $p < 0.001$.

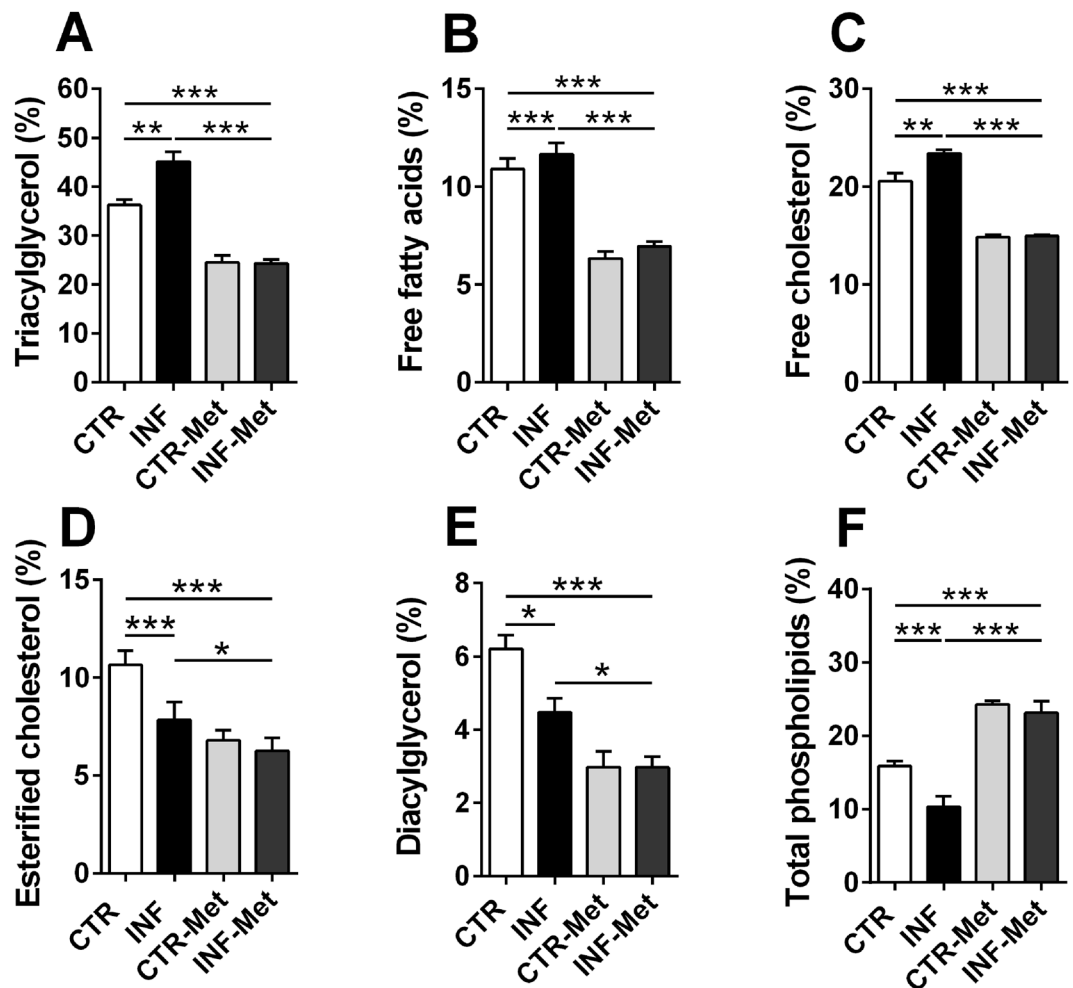


Figure 7. Effect of metformin pretreatment on the hepatic lipid profile of mice infected with *P. chabaudi*. The graphs show lipid classes obtained by thin-layer chromatography and percentages determined using densitometric analysis. White bars indicate controls (CTR, $n = 9$), black bars indicate the infected group (INF, $n = 9$), light gray bars indicate the metformin pretreated controls (CTR-Met, $n = 9$), and dark gray bars indicate the metformin pretreated infected group (INF-Met, $n = 7$). Statistical analyses: one-way ANOVA followed by Dunnett's multiple comparisons test. Values are presented as mean \pm standard error. ** $p < 0.01$ and *** $p < 0.001$.

Thus, IL-10 appears to play a critical role in regulating the effects of TNF during malaria, but at the same time, IL-10 may promote high-density infections that result in other complications, including accumulation of infected red blood cells in tissue that can cause hypoxia and direct damage to the vasculature^{23,24}.

P. chabaudi promoted hypocholesterolemia, hypertriglyceridemia, hypoglycemia, hyperproteinemia, and altered profile of cytokines, which clearly indicated plasma lipid dysregulation and increased proinflammatory response that is consistent with previous studies^{25–29}. However, we also discovered that these plasma changes are accompanied by alterations in the lipid profile of WAT and with increased percentages of TAG and SM; to our knowledge, this is the first time that these effects have been reported in the literature. Considering that infected erythrocytes adhere to capillary endothelial cells in multiple tissues (including WAT³⁰), it is possible that the parasite acts indirectly on the adipocytes from the endothelium and stimulates lipid accumulation to benefit from these lipids for its development and multiplication in the host. Further studies are needed to better understand the molecular pathways involved in this regulation and to address its relevance to host–parasite interactions.

Our study was focused on the liver because this tissue possess the complete set of enzymatic machinery necessary to synthesize lipids, since it is the main organ for lipid exchange in the body^{31,32}. Liver from infected mice exhibited increased percentages of TAG, free fatty acids, and free cholesterol, suggestive of hepatic dyslipidemia, and our quantitative polymerase chain reaction (qPCR) results corroborated this by revealing a decreased hepatic mRNA expression of PPAR- α , PGC-1 α , and CPT1-A during infection. PPAR- α is the most abundant transcription factor in healthy livers. It is responsible for activating fatty acid uptake and oxidation, and PPAR- α hepatocyte-specific knockout impairs free fatty acid homeostasis and affects the entire body in fed or fasting mice³³. PGC-1 α is a transcriptional coactivator induced by fasting, and it activates fatty acid oxidation and gluconeogenesis via PPAR- α , FoxO1, and HNF-4 α stimulation^{34–36}. CPT1-A is a key enzyme in the β -oxidation

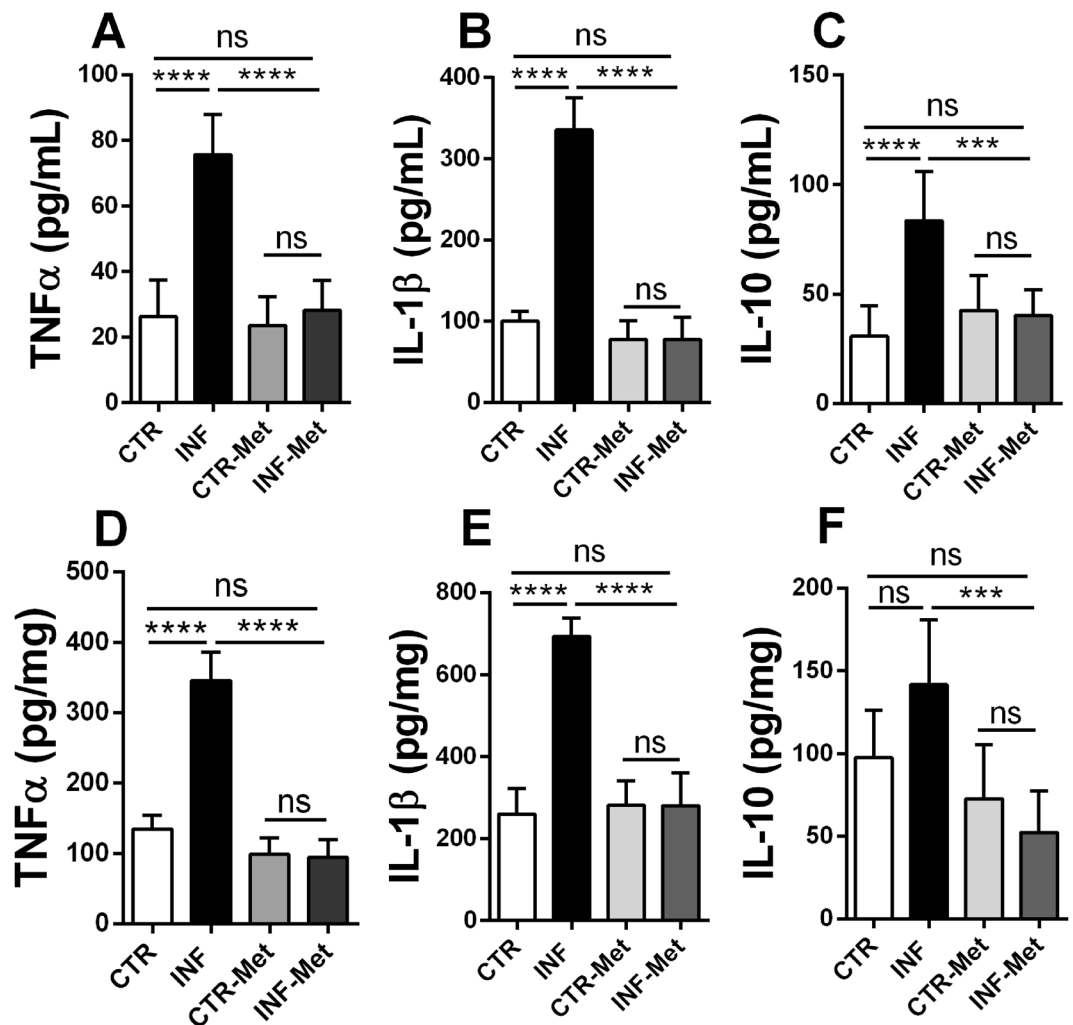


Figure 8. Effect of pretreatment of metformin on cytokines profile measured on plasma and liver of Swiss mice. The graphs shows the concentration of TNF α , IL-1 β , and IL-10 obtained by ELISA assay. White bars indicate controls (CTR, $n = 9$), black bars indicate the infected group (INF, $n = 9$), light gray bars indicate the metformin pretreated controls (CTR-Met, $n = 9$), and dark gray bars indicate the metformin pretreated infected group (INF-Met, $n = 7$). Statistical analyses: one-way ANOVA followed by Dunnett's multiple comparisons test. Values are presented as mean \pm standard error. ** $p < 0.01$ and *** $p < 0.001$.

process and is regulated not only by malonyl-CoA, but also by thyroid hormone and insulin^{37,38}. Together, our results all point to a lower fatty acid oxidation state in infected compared to healthy livers.

In contrast, we observed an increased hepatic mRNA and protein expression of PPAR- γ and FAS in infected compared to control mice. FAS is key enzyme in the process of fatty acid synthesis, and its knockout in mice is lethal, indicating a crucial role for *de novo* lipogenesis in embryonic development³⁹. PPAR- γ is a transcriptional regulator of hepatic fatty acid storage, and its liver-specific knockout in obese mice reduces lipid accumulation⁴⁰. Thus, the increase in PPAR- γ and FAS gene expression implies increased lipid biosynthesis during infection.

The enzyme AMPK is a central regulator of the biosynthesis and degradation of lipids, carbohydrates, and proteins⁴¹. Here we showed that hepatic AMPK is strongly regulated during *Plasmodium* infection, which decreases AMPK phosphorylation and leads to the activation of an anabolic state (Figs 4A and S1A). ACC, SREBP-1c, and PPAR α are also essential in controlling lipid synthesis/degradation pathways, and they are targets for AMPK phosphorylation^{42,43}. *Plasmodium* infection decreased ACC, and SREBP-1c phosphorylation (i.e., induced their activation) (Figs 4B,C and S1B,C) and decreased PPAR α phosphorylation (i.e., decrease their activation) (Figs 4E and S1E). In addition, infection increased the protein expression of FAS and PPAR γ (Figs 4D,F and S1D,F). FAS is stimulated by SREBP-1c⁴⁴, resulting in favored lipogenesis over lipolysis during infection.

Metformin is a classic AMPK activator and is the most widely prescribed drug for treating hyperglycemia in patients with type 2 diabetes mellitus (T2DM)⁴⁵. It has also been used for prevention in prediabetic populations^{46,47}, for avoiding vascular complications associated with T2DM⁴⁸, and for reducing inflammation and hepatic steatosis⁴⁹. Malaria has been associated with T2DM previously⁵⁰. A case-control study conducted in Ghana reported that patients with T2DM had a 46% increased risk of infection with *P. falciparum*⁵¹ due to impaired defense against liver and blood-stage parasites, decreased T-cell mediated immunity, and increased

glucose availability for the parasites⁵². Recent work has shown that maintaining glycemia is essential for tolerance to murine malaria, since severe hypoglycemia contributes to increased brain inflammation and increased lethality of infected mice^{53,54}. The use of metformin by T2DM patients significantly reduces the incidence of malaria infection compared to those not on metformin treatment⁵⁵. In addition, metformin has been shown to reduce *P. falciparum* prevalence and to exhibit synergistic effects with antimalarial drugs, including atovaquone^{51,56}, and the combination of artesunate/esomeprazole – which was even more effective in reducing glucose levels and attenuating metabolic syndrome symptoms, promoting effective parasite clearance and preventing its recrudescence than the metformin alone⁵⁷.

In this study, we showed that pretreatment with metformin protected *P. chabaudi* infected mice from developing clinically significant malaria. The role of AMPK in infection severity has been previously studied in viral infections⁵⁸ and malaria⁵⁹; however, the latter study was performed during the malaria hepatic cycle. Our study consists of a distinct and novel experimental design, which was used to address the *Plasmodium* intraerythrocytic cycle, where the parasite no longer infects hepatocytes and malarial signs and symptoms are more intense. Thus, we have demonstrated here that malarial disease may be preventable by pretreatment with metformin.

The mechanisms by which metformin pretreatment inhibits *Plasmodium* infection still need to be determined. We suggest, however, that the lipogenic state induced by AMPK downregulation favors *Plasmodium* multiplication and dissemination within the mammal host, while metformin-induced AMPK activation limits the lipid supply to the parasite, thereby impairing infection. Pathogens extensively utilize their hosts' cellular lipidome pathways, and over millions of years of parasitism they have evolved very sophisticated mechanisms to lengthen their lifespans in their hosts. The acquisition of host lipids is critical in modulating host–pathogen interactions and in improving the pathogens' virulence⁶⁰. Lipids are an energy source for the pathogens, which cannot synthesize fatty acids, and so they rely on the acquisition of these molecules from the host and subsequent induction of β -oxidation⁶¹. In the case of *Plasmodium*, acquisition of host lipids is fundamental and particularly important for the intraerythrocytic stage, when this parasite loses the ability to synthesize fatty acids and is only capable of storing lipids within its parasitophorous vacuole⁶². Furthermore, host lipids provide building blocks for pathogen assembly^{63–65} and a convenient carbon source, as has been described for *Mycobacterium tuberculosis*^{66,67}, *Salmonella*⁶⁸, *Candida albicans*⁶⁹, and *Cryptococcus neoformans*⁷⁰.

Pretreatment with metformin significantly decreased the concentration of TNF α , IL-1 β , and IL-10 in infected compared to noninfected mice (Fig. 8). Metformin has been shown to attenuate proinflammatory response in several diseases^{71–73}. Therefore, metformin-induced AMPK activation suppresses the uncontrolled inflammation triggered by the presence of the parasite in the blood, protecting the liver from injury and consequent lipid accumulation, which will culminate with inhibition of the development and multiplication of *Plasmodium* in the blood.

Figure 9 shows a working model of the molecular mechanisms involved in *Plasmodium* infection, indicating a possible route that elicits the accumulation of hepatic lipids during infection in mice. Reduced AMPK activation leads to elevated ACC activation, which stimulates lipid synthesis, and to reduced lipid oxidation due to the inhibition of CPT1-A, a β -oxidation rate-limiting enzyme. Lower AMPK also leads to increased SREBP-1c activation, which stimulates the transcription of genes involved in lipid synthesis, such as FAS. A complementary axis supporting this pathway converges from the increased protein expression of PPAR γ , a transcription factor involved on lipid synthesis and decreased phosphorylation levels of PPAR α and mRNA expression of PGC-1 α , both fatty acid oxidation inducers⁷⁴. Metformin activates hepatic AMPK and inhibits ACC activity, possibly reversing all the signaling pathways that contributed to lipid accumulation in the liver during *Plasmodium* infection in mice. In summary, the data we have presented suggest that AMPK represents an attractive target for new drugs for the prevention and treatment of malaria.

Materials and Methods

Parasites and mice. Parasites and mice were obtained from the Laboratory of Ultrastructure and Cellular Biology Hertha Meyer, Carlos Chagas Filho Institute of Biophysics of the Federal University of Rio de Janeiro, in collaboration with Dr. Kildare Miranda. *P. chabaudi* parasites were maintained by successive weekly passages in Swiss mice prior to the experimental infection protocol. Eight-week-old male Swiss mice were kept in a 12 h/12 h light/dark cycle and with water and food *ad libitum*.

Ethics statement. All animals were treated according to the *Guide for the Care and Use of Laboratory Animals*⁷⁵, and all experimental protocols were approved by the Federal University of Rio de Janeiro and the Center for Health Sciences Animal Care Committee (Protocol IBCCF209-09/16).

Experimental design 1. Male Swiss mice (~25 g, 8-weeks old) were separated into infected (INF, $n = 14$) and control (CTR, $n = 14$) groups. Infective inocula (1×10^6 RBCs containing *P. chabaudi*) were then prepared and intraperitoneally injected into the INF group. CTR mice received similar inocula but lacking the parasite (1×10^6 uninfected RBCs). After injection, parasitemia was monitored using daily blood smears fixed and stained with the Fast Panoptic method (Laborclin[®]). When parasitemia of INF animals reached 80% (five days after infection), all mice were euthanized in a CO₂ chamber and blood was collected into vials containing 3% sodium citrate as an anticoagulant agent after cardiac puncture. Livers and retroperitoneal WAT were collected and stored in a liquid nitrogen tank. Blood samples were centrifuged at 500 g for 15 min for plasma collection and then stored at –20 °C until needed for analysis.

Experimental design 2. Male Swiss mice (~25 g, 8-weeks old) were separated into four groups: control (CTR, $n = 9$), infected (INF, $n = 9$), pretreated with metformin (CTR-Met, $n = 9$), and infected and pretreated

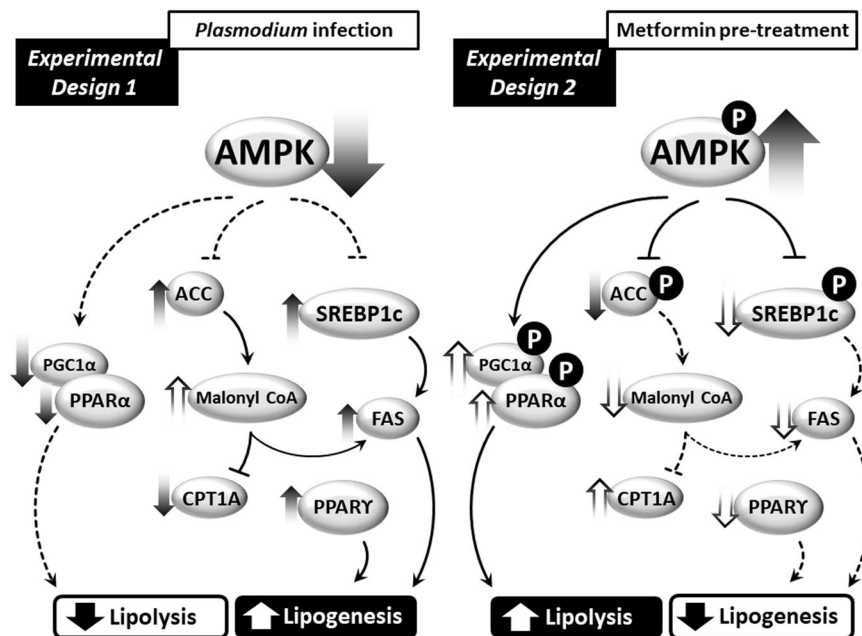


Figure 9. A working model for the role of the enzyme AMPK in regulating lipid metabolism during *P. chabaudi* infection. *P. chabaudi* infection induces a decrease in active hepatic AMPK, which leads to the activation of ACC and SREBP-1c and subsequent stimulation of gene transcription and expression of proteins involved in lipid biosynthesis, such as the enzyme FAS. Concomitantly, there is a reduction of β -oxidation due to the inhibition of the β -oxidation-limiting enzyme CPT1-A and decreased expression of PPAR- α and PGC-1 α . Pretreatment with metformin elicits the activation of hepatic AMPK, reversing the lipid metabolism perturbations observed following *Plasmodium* infection and preventing the efficiency of *Plasmodium* infection of mice.

with metformin (INF-Met, $n = 9$). Groups CTR-Met and INF-Met were pretreated with metformin (150 mg/kg) intraperitoneally once a day for 21 days⁷⁶. Groups CTR and INF underwent similar treatment, but with 0.15 M NaCl instead. Animals were then injected intraperitoneally with the infective inoculum (1×10^6 RBCs containing *P. chabaudi* for groups INF and INF-Met) or uninfected inoculum (1×10^6 healthy RBCs for groups CTR and CTR-Met). Parasitemia was monitored by daily blood smears stained with the Fast Panoptic method (Laborclin[®]). Mice were euthanized when the parasitemia of the INF group reached 80% (five days after infection). Blood and tissue samples were collected and stored using the same procedures as in Experimental Design 1.

Lipid extraction and analysis. Lipid extraction was performed using a methodology modified from Bligh and Dyer (1959)⁷⁷. Liver and WAT samples (10 mg) were added to a 500 μ L of lysis buffer (50 mM Tris-HCl, pH 7.4, 1% NP-40, 250 mM NaCl, 5 mM EDTA, and 50 mM NaF), homogenized, and centrifuged at 2,500 g for 5 min. Supernatants were added to glass conical tubes along with a 4 mL of chloroform-methanol-water solution (2:1:0.8 mL) and shaken intermittently for 2 h. Extracts were then centrifuged at 730 g for 20 min at 4 °C in a High-Speed Refrigerated Centrifuge (Hitachi, Ltd., TO, Japan). The supernatant was collected, and 2 mL of water and chloroform (1:1 mL) were added, and the solution was centrifuged at 730 g for 20 min at 4 °C prior to collection of the organic phase (containing lipids). The extracted lipids were analyzed by thin-layer chromatography (TLC) using a hexane/diethyl ether/acetic acid solvent (60:40:1 v/v)⁷⁸. To visualize the lipids, plates were immersed in a carbonization solution consisting of 8% CuSO₄ and 10% H₃PO₄ for 10 s and heated at 110 °C for 20 min⁷⁹. Plates were analyzed by densitometry using ImageMaster TotalLab software (TotalLab, Newcastle, UK).

Colorimetric enzyme assays. Plasma TAG, total cholesterol, and glucose concentrations were determined using commercial enzyme kits (Doles[®], Goiânia, Brazil) and by following the manufacturers' instructions.

Protein concentration determination. Plasma protein concentration was determined by the Lowry method⁸⁰, using bovine serum albumin (0.1%) as a standard.

RNA extraction and cDNA synthesis. Liver samples (10 mg) were homogenized in 500 μ L TRIzol reagent (Invitrogen Corporation, Carlsbad, CA, USA) and centrifuged at 7,500 g for 15 min at 4 °C. The supernatant was transferred to microtubes containing 200 μ L of chloroform (Merck, Darmstadt, Germany). Samples were shaken for 10 s and centrifuged again at 7,500 g for 15 min at 4 °C. Supernatants were collected and transferred to new microtubes containing 200 μ L of isopropanol (Merck). Samples were mixed gently by inversion and incubated at room temperature for 10 min and then centrifuged at 7,500 g for 15 min at 4 °C. The supernatants were discarded, and the precipitate was resuspended in 200 μ L of absolute ethanol. Samples were then centrifuged at 3,000 g at 4 °C for 15 min, the supernatants were discarded, and the pellets were resuspended in 30 μ L of RNase-free water. The RNA concentration was quantified by spectrophotometry using a NanoDrop (Thermo Scientific, Wilmington, NC, USA).

cDNA synthesis was performed using a High-Capacity cDNA Reverse Transcription kit (Applied Biosystems, Foster City, CA, USA). Reactions contained 1 µg of RNA, 2 µL of reaction buffer, 0.8 µL of 100 µM dNTPs, 2 µL of random primers, 1 µL of 50 U/µL reverse transcriptase, and RNase-free water sufficient for a final volume of 22 µL. The reaction was incubated for 10 min at 25 °C and then at 37 °C for 2 h. Samples were stored at –20 °C until use.

Quantitative polymerase chain reaction (qPCR). qPCR was performed using StepOne Real-Time PCR System (Applied Biosystems, Thermo Fisher Scientific, Waltham, MA, USA) and a Power SYBR® Green PCR Master kit (Applied Biosystems, Thermo Fisher Scientific). Primers were custom-designed (Table 1), validated using the Primer-BLAST webpage from the National Center for Biotechnology Information (www.ncbi.nlm.nih.gov/tools/primer-blast), and synthesized by Integrated DNA Technologies (Coralville, IA, USA). 5 µL of the cDNA sample was mixed with 0.9 µL of forward and reverse primers mix (0.05 µg/µL), 0.35 µL of dH₂O, and 6.25 µL of SYBR® Green Master Mix, reaching a final volume of 12.5 µL. Ninety-six-well optical plates were run in the thermocycler using the following parameters: 50 °C for 2 min, 95 °C for 10 min, and 40 cycles of 95 °C for 15 s, 60 °C for 30 s, and 72 °C for 45 s, followed by a melting curve. Relative mRNA expression was calculated by the 2^{–ΔΔCT} method⁸¹, and *Rplp0* was used as an endogenous control.

Immunoblots. Liver samples (50 mg) were homogenized in a lysis buffer (50 mM Tris-HCl, pH 7.4, 1% NP-40, 250 mM NaCl, 5 mM EDTA, and 50 mM NaF) containing protease inhibitor cocktail (catalog number P8340, Sigma Chemicals, St. Louis, MO, USA), and protein was quantified by the Lowry method⁸⁰. Extracts (60 µg) were electrophoresed in 10% SDS-PAGE gels, transferred to nitrocellulose membranes (GE Healthcare Life Sciences, Marlborough, MA, USA), and blocked for 1 h with TBS-Tween (20 mM Tris-HCl, pH 7.5, 500 mM NaCl, and 0.1% Tween 20) containing 3% bovine serum albumin. Membranes were subsequently probed with anti-β-actin monoclonal mouse antibody (1: 1000, Santa Cruz, CA, USA), polyclonal rabbit anti-phospho-AMPK (1: 500, Santa Cruz, CA, USA), polyclonal rabbit anti-AMPK (1: 500, Santa Cruz, CA, USA), monoclonal rabbit anti-phospho-SREBP-1c (Abcam, MA, USA), polyclonal rabbit anti-SREBP-1c (1: 500, Santa Cruz, CA, USA), polyclonal rabbit anti-ACC (1: 500, Santa Cruz, CA, USA), monoclonal rabbit anti-phospho-ACC (1: 500, Abcam), and polyclonal rabbit anti-FAS (1: 500, Santa Cruz, CA, USA), anti-PPAR_γ (1:1000, Santa Cruz, CA, USA), anti-phospho-PPAR_α (1:1000, Santa Cruz, CA, USA), and anti-PPAR_α (1:1000, Santa Cruz, CA, USA). Membranes were incubated for 90 min with anti-rabbit or anti-mouse polyclonal antibody conjugated to horseradish peroxidase (HRP; 1: 20000, Santa Cruz, CA, USA). Immunoreactive proteins were visualized by chemiluminescence using an ECL kit (Amersham Pharmacia, GE Healthcare Life Sciences) and detected with an Image Quant LAS 4000 (GE Healthcare Life Sciences, Marlborough, MA, USA). Densitometric quantitative analysis was conducted using ImageMaster TotalLab software (TotalLab).

Cytokines measurements. TNF_α, IL-1_β, and IL-10 cytokines analysis was performed on plasma and liver samples. The protocol used followed the manufacturer's specifications (R&D, Systems Corporation, Minneapolis, MN). Briefly, 96-well microplates were sensitized with anti-TNF_α, IL-1_β, and IL-10 monoclonal antibodies, diluted in PBS and incubated for 24 hours at room temperature. The plates were blocked with PBS/4% bovine albumin serum (SAB-Sigma Chemicals, St. Louis, MO, USA) and incubated for 2 hours at room temperature. After following three wash cycles with 0.05% PBS-Tween-20 buffer, samples and standard curve serial dilutions were added to the plates and incubated for 1 hour at room temperature. Thereafter, biotin-conjugated antibodies were added to the plates and incubated for 1 hour. Following, streptavidin peroxidase was added for 20 minutes. After further 3 wash cycles, the 3', 3', 5, 5' tetramethylbenzidine substrate (TmB, Zymed) was added to the plates and the reaction was stopped by addition of sulfuric acid 1 M. The plates were read using an ELISA microplate reader at 450 nm.

Statistical analysis. Statistical analyses were performed using GraphPad Prism software version 6.0 (GraphPad Inc., CA, USA) and included unpaired Student's *t*-test, one-way ANOVA followed by Dunnett's multiple comparisons test, and two-way ANOVA followed by Tukey's multiple comparisons test. Specific statistical analyses are described in the figures' legends. Results are expressed as mean ± standard error, and differences were considered significant when *p* < 0.05.

Data Availability

All data generated or analysed during this study are included in this published article (and its Supplementary Information Files).

References

- Rodrigues, P. T. *et al.* Human migration and the spread of malaria parasites to the New World. *Sci. Rep.* **8**, 1993 (2018).
- Li, J.-L. *et al.* Current advance in cerebral malaria. *Zhongguo Zhong Yao Za Zhi* **42**, 4548–4555 (2017).
- Health Organization, W. *World Malaria Report 2016*.
- WHO|World malaria report 2017. *WHO* (2018).
- Taylor, T. & Agbenyega, T. Malaria. In *Hunter's Tropical Medicine and Emerging Infectious Disease* 695–717 (Elsevier), <https://doi.org/10.1016/B978-1-4160-4390-4.00096-5> (2013).
- Clark, I. A., Budd, A. C., Allea, L. M. & Cowden, W. B. Human malarial disease: a consequence of inflammatory cytokine release. *Malar. J.* **5**, 85 (2006).
- Miller, L. H., Ackerman, H. C., Su, X. & Wellems, T. E. Malaria biology and disease pathogenesis: insights for new treatments. *Nat. Med.* **19**, 156–167 (2013).
- Schofield, L. & Grau, G. E. Immunological processes in malaria pathogenesis. *Nat. Rev. Immunol.* **5**, 722–735 (2005).
- Wunderlich, F., Al-Quraishy, S. & Dkhil, M. A. Liver-inherent immune system: its role in blood-stage malaria. *Front. Microbiol.* **5**, 559 (2014).
- Rupani, A. B. & Amarapurkar, A. D. Hepatic changes in fatal malaria: an emerging problem. *Ann. Trop. Med. Parasitol.* **103**, 119–127 (2009).
- Anand, A. C. & Puri, P. Jaundice in malaria. *J. Gastroenterol. Hepatol.* **20**, 1322–1332 (2005).

12. van den Berghe, G. The role of the liver in metabolic homeostasis: Implications for inborn errors of metabolism. *J. Inherit. Metab. Dis.* **14**, 407–420 (1991).
13. Woods, A. *et al.* Liver-Specific Activation of AMPK Prevents Steatosis on a High-Fructose Diet. *Cell Rep.* **18**, 3043–3051 (2017).
14. Beg, Z. H., Allmann, D. W. & Gibson, D. M. Modulation of 3-hydroxy-3-methylglutaryl coenzyme A reductase activity with cAMP and with protein fractions of rat liver cytosol. *Biochem. Biophys. Res. Commun.* **54**, 1362–9 (1973).
15. Sim, A. T. & Hardie, D. G. The low activity of acetyl-CoA carboxylase in basal and glucagon-stimulated hepatocytes is due to phosphorylation by the AMP-activated protein kinase and not cyclic AMP-dependent protein kinase. *FEBS Lett.* **233**, 294–8 (1988).
16. Clarke, P. R. & Hardie, D. G. Regulation of HMG-CoA reductase: identification of the site phosphorylated by the AMP-activated protein kinase *in vitro* and in intact rat liver. *EMBO J.* **9**, 2439–46 (1990).
17. Ha, J., Lee, J. K., Kim, K. S., Witters, L. A. & Kim, K. H. Cloning of human acetyl-CoA carboxylase-beta and its unique features. *Proc. Natl. Acad. Sci. USA* **93**, 11466–70 (1996).
18. Abu-Elheiga, L., Almaraz-Ortega, D. B., Baldini, A. & Wakil, S. J. Human acetyl-CoA carboxylase 2. Molecular cloning, characterization, chromosomal mapping, and evidence for two isoforms. *J. Biol. Chem.* **272**, 10669–77 (1997).
19. McGarry, J. D., Leatherman, G. F. & Foster, D. W. Carnitine palmitoyltransferase I. The site of inhibition of hepatic fatty acid oxidation by malonyl-CoA. *J. Biol. Chem.* **253**, 4128–36 (1978).
20. Hardie, D. G. How cells sense energy. *Nature* **472**, 176–177 (2011).
21. Shaffer, N. *et al.* Tumor Necrosis Factor and Severe Malaria. *J. Infect. Dis.* **163**, 96–101 (1991).
22. Day, N. P. J. *et al.* The Prognostic and Pathophysiologic Role of Pro- and Antiinflammatory Cytokines in Severe Malaria. *J. Infect. Dis.* **180**, 1288–1297 (1999).
23. Li, C., Corraliza, I. & Langhorne, J. A defect in interleukin-10 leads to enhanced malarial disease in Plasmodium chabaudi chabaudi infection in mice. *Infect. Immun.* **67**, 4435–42 (1999).
24. Freitas do Rosario, A. P. & Langhorne, J. T cell-derived IL-10 and its impact on the regulation of host responses during malaria. *Int. J. Parasitol.* **42**, 549–555 (2012).
25. Haldar, K., Murphy, S. C., Milner, D. A. & Taylor, T. E. Malaria: mechanisms of erythrocytic infection and pathological correlates of severe disease. *Annu. Rev. Pathol.* **2**, 217–49 (2007).
26. Brugat, T. *et al.* Sequestration and histopathology in Plasmodium chabaudi malaria are influenced by the immune response in an organ-specific manner. *Cell. Microbiol.* **16**, 687–700 (2014).
27. Barthélémy, M., Vuong, P. N., Gabrion, C. & Petit, G. Plasmodium chabaudi chabaudi chronic malaria and pathologies of the urogenital tract in male and female BALB/c mice. *Parasitology* **128**, 113–22 (2004).
28. Elased, K. & Playfair, J. H. Hypoglycemia and hyperinsulinemia in rodent models of severe malaria infection. *Infect. Immun.* **62**, 5157–60 (1994).
29. Elased, K. M., de Souza, J. B. & Playfair, J. H. Reversal of type 2 diabetes in mice by products of malaria parasites: I. Effect of inactivated parasites. *Metabolism.* **49**, 937–41 (2000).
30. Franke-Fayard, B., Fonager, J., Braks, A., Khan, S. M. & Janse, C. J. Sequestration and tissue accumulation of human malaria parasites: can we learn anything from rodent models of malaria? *PLoS Pathog.* **6**, e1001032 (2010).
31. Rui, L. Energy Metabolism in the Liver. In *Comprehensive Physiology* **4**, 177–197 (John Wiley & Sons, Inc., 2014).
32. Jump, D. B. Fatty acid regulation of hepatic lipid metabolism. *Curr. Opin. Clin. Nutr. Metab. Care* **14**, 115–20 (2011).
33. Montagner, A. *et al.* Liver PPAR α is crucial for whole-body fatty acid homeostasis and is protective against NAFLD. *Gut* **65**, 1202–14 (2016).
34. Lin, J., Handschin, C. & Spiegelman, B. M. Metabolic control through the PGC-1 family of transcription coactivators. *Cell Metab.* **1**, 361–370 (2005).
35. Puigserver, P. Tissue-specific regulation of metabolic pathways through the transcriptional coactivator PGC1- α . *Int. J. Obes. (Lond)*. **29**(Suppl 1), S5–9 (2005).
36. Finck, B. N. & Kelly, D. P. PGC-1 coactivators: inducible regulators of energy metabolism in health and disease. *J. Clin. Invest.* **116**, 615–22 (2006).
37. McGarry, J. D. & Brown, N. F. The mitochondrial carnitine palmitoyltransferase system. From concept to molecular analysis. *Eur. J. Biochem.* **244**, 1–14 (1997).
38. Saggerson, E. D. & Carpenter, C. A. Effects of fasting, adrenalectomy and streptozotocin-diabetes on sensitivity of hepatic carnitine acyltransferase to malonyl CoA. *FEBS Lett.* **129**, 225–8 (1981).
39. Chirala, S. S. *et al.* Fatty acid synthesis is essential in embryonic development: fatty acid synthase null mutants and most of the heterozygotes die in utero. *Proc. Natl. Acad. Sci. USA* **100**, 6358–63 (2003).
40. Matsusue, K. *et al.* Liver-specific disruption of PPAR γ in leptin-deficient mice improves fatty liver but aggravates diabetic phenotypes. *J. Clin. Invest.* **111**, 737–47 (2003).
41. Jeon, S.-M. Regulation and function of AMPK in physiology and diseases. *Exp. Mol. Med.* **48**, e245–e245 (2016).
42. Hardie, D. G. Regulation of fatty acid and cholesterol metabolism by the AMP-activated protein kinase. *Biochim. Biophys. Acta - Lipids Lipid Metab.* **1123**, 231–238 (1992).
43. Li, Y. *et al.* AMPK phosphorylates and inhibits SREBP activity to attenuate hepatic steatosis and atherosclerosis in diet-induced insulin-resistant mice. *Cell Metab.* **13**, 376–388 (2011).
44. Xu, X., So, J.-S., Park, J.-G. & Lee, A.-H. Transcriptional control of hepatic lipid metabolism by SREBP and ChREBP. *Semin. Liver Dis.* **33**, 301–11 (2013).
45. Lipscombe, L. *et al.* 2018 Clinical Practice Guidelines Pharmacologic Glycemic Management of Type 2 Diabetes in Adults Diabetes Canada Clinical Practice Guidelines Expert Committee. *Can. J. Diabetes* **42**, 88–103 (2015).
46. Knowler, W. C. *et al.* Reduction in the incidence of type 2 diabetes with lifestyle intervention or metformin. *N. Engl. J. Med.* **346**, 393–403 (2002).
47. Balani, J., Hyer, S., Johnson, A. & Shehata, H. Pregnancy outcomes after metformin treatment for gestational diabetes: a case-control study. *Obstet. Med.* **5**, 78–82 (2012).
48. Roussel, R. *et al.* Metformin use and mortality among patients with diabetes and atherothrombosis. *Arch. Intern. Med.* **170**, 1892–9 (2010).
49. Nair, S., Diehl, A. M., Wiseman, M., Farr, G. H. & Perrillo, R. P. Metformin in the treatment of non-alcoholic steatohepatitis: a pilot open label trial. *Aliment. Pharmacol. Ther.* **20**, 23–28 (2004).
50. Okell, L. C., Ghani, A. C., Lyons, E. & Drakeley, C. J. Submicroscopic Infection in Plasmodium falciparum –Endemic Populations: A Systematic Review and Meta-Analysis. *J. Infect. Dis.* **200**, 1509–1517 (2009).
51. Danquah, I., Bedu-Addo, G. & Mockenhaupt, F. P. Type 2 diabetes mellitus and increased risk for malaria infection. *Emerg. Infect. Dis.* **16**, 1601–4 (2010).
52. Muller, L. M. A. J. *et al.* Increased Risk of Common Infections in Patients with Type 1 and Type 2 Diabetes Mellitus. *Clin. Infect. Dis.* **41**, 281–288 (2005).
53. Vandermosten, L. *et al.* Adrenal hormones mediate disease tolerance in malaria. *Nat. Commun.* **9**, 4525 (2018).
54. Cumnock, K. *et al.* Host Energy Source Is Important for Disease Tolerance to Malaria. *Curr. Biol.* **28**, 1635–1642.e3 (2018).
55. Alves, C., Casqueiro, J. & Casqueiro, J. Infections in patients with diabetes mellitus: A review of pathogenesis. *Indian J. Endocrinol. Metab.* **16**, 27 (2012).
56. Jones, K. & Ward, S. A. Biguanide-atovaquone synergy against Plasmodium falciparum *in vitro*. *Antimicrob. Agents Chemother.* **46**, 2700–3 (2002).

57. Oriaino, S. E. Effect of a Poly-Pill of Metformin, Artesunate and Esomeprezole low-dose (MEALD) combination in prevention of Malaria and selected metabolic syndrome criteria. *World J. Pharm. Life Sci.* **4**, 1–10 (2018).
58. Moser, T. S., Schieffer, D. & Cherry, S. AMP-activated kinase restricts Rift Valley fever virus infection by inhibiting fatty acid synthesis. *PLoS Pathog.* **8**, e1002661 (2012).
59. Ruivo, M. T. G. *et al.* Host AMPK Is a Modulator of Plasmodium Liver Infection. *Cell Rep.* **16**, 2539–2545 (2016).
60. Peterson, K. M. & Alderete, J. F. Trichomonas vaginalis is dependent on uptake and degradation of human low density lipoproteins. *J. Exp. Med.* **160**, 1261–72 (1984).
61. Hansmeier, N. *et al.* A comprehensive proteome map of the lipid-requiring nosocomial pathogen *Corynebacterium jeikeium* K411. *Proteomics* **7**, 1076–96 (2007).
62. Coppens, I. & Vielemeyer, O. Insights into unique physiological features of neutral lipids in Apicomplexa: from storage to potential mediation in parasite metabolic activities. *Int. J. Parasitol.* **35**, 597–615 (2005).
63. Lin, M. & Rikihisa, Y. Ehrlichia chaffeensis and Anaplasma phagocytophilum lack genes for lipid A biosynthesis and incorporate cholesterol for their survival. *Infect. Immun.* **71**, 5324–31 (2003).
64. Heung, L. J., Luberto, C. & Del Poeta, M. Role of Sphingolipids in Microbial Pathogenesis. *Infect. Immun.* **74**, 28–39 (2006).
65. Nishikawa, Y. *et al.* Host cell lipids control cholesteryl ester synthesis and storage in intracellular Toxoplasma. *Cell. Microbiol.* **7**, 849–67 (2005).
66. Schaible, U. E. & Kaufmann, S. H. E. A nutritive view on the host-pathogen interplay. *Trends Microbiol.* **13**, 373–80 (2005).
67. Pandey, A. K. & Sassetti, C. M. Mycobacterial persistence requires the utilization of host cholesterol. *Proc. Natl. Acad. Sci. USA* **105**, 4376–80 (2008).
68. Fang, F. C., Libby, S. J., Castor, M. E. & Fung, A. M. Isocitrate lyase (AceA) is required for Salmonella persistence but not for acute lethal infection in mice. *Infect. Immun.* **73**, 2547–9 (2005).
69. Prigneau, O. *et al.* Genes involved in β -oxidation, energy metabolism and glyoxylate cycle are induced by *Candida albicans* during macrophage infection. *Yeast* **20**, 723–730 (2003).
70. Rude, T. H., Toffaletti, D. L., Cox, G. M. & Perfect, J. R. Relationship of the glyoxylate pathway to the pathogenesis of *Cryptococcus neoformans*. *Infect. Immun.* **70**, 5684–94 (2002).
71. Saisho, Y. Metformin and Inflammation: Its Potential Beyond Glucose-lowering Effect. *Endocr. Metab. Immune Disord. Drug Targets* **15**, 196–205 (2015).
72. Cameron, A. R. *et al.* Anti-Inflammatory Effects of Metformin Irrespective of Diabetes Status. *Circ. Res.* **119**, 652–65 (2016).
73. Abbaszadeh, A., Koushki, S., Koushki, S., Eskandarzadeh, M. & Hasanvand, A. Metformin; a mini-review to its antioxidative and anti-inflammatory properties. *J. Ren. Inj. Prev.* **7**, 7–10 (2017).
74. Fan, W. & Evans, R. PPARs and ERRs: molecular mediators of mitochondrial metabolism. *Curr. Opin. Cell Biol.* **33**, 49–54 (2015).
75. Clark, J. D., Gebhart, G. F., Gonder, J. C., Keeling, M. E. & Kohn, D. F. The 1996 Guide for the Care and Use of Laboratory Animals. *ILARJ.* **38**, 41–48 (1997).
76. Calvert, J. W. *et al.* Acute metformin therapy confers cardioprotection against myocardial infarction via AMPK-eNOS-mediated signaling. *Diabetes* **57**, 696–705 (2008).
77. Bligh, E. G. & Dyer, W. J. A rapid method of total lipid extraction and purification. *Can. J. Biochem. Physiol.* **37**, 911–917 (1959).
78. Elliott, R. J., Moore, G. W. & Biggart, J. D. Human aortic lipids: extraction, fractionation and identification. *Biochem. Soc. Trans.* **13**, 471–472 (1985).
79. Ruiz, J. I. & Ochoa, B. Quantification in the subnanomolar range of phospholipids and neutral lipids by monodimensional thin-layer chromatography and image analysis. *J. Lipid Res.* **38**, 1482–9 (1997).
80. Lowry, O. H., Rosebrough, N. J., Farr, A. L. & Randall, R. J. Protein measurement with the Folin phenol reagent. *J. Biol. Chem.* **193**, 265–75 (1951).
81. Livak, K. J. & Schmittgen, T. D. Analysis of relative gene expression data using real-time quantitative PCR and the 2(-Delta Delta C(T)) Method. *Methods* **25**, 402–8 (2001).

Acknowledgements

We would like to express our gratitude to Mileane S. Busch for excellent technical assistance. This work was carried out with funding from Fundação Carlos Chagas Filho de Amparo à Pesquisa do Estado do Rio de Janeiro (FAPERJ), Conselho Nacional de Desenvolvimento Científico e Tecnológico (CNPq), Coordenação de Aperfeiçoamento de Pessoal de Nível Superior (CAPES) and Instituto Nacional de Ciência e Tecnologia - Entomologia Molecular (INCT-EM).

Author Contributions

Conceived and designed the experiments: G.C.A. and G.E.G.K. Performed the experiments: G.E.G.K., C.H.C.W., M.F.C.A., I.R. and T.C.A. Analyzed the data: G.E.G.K. and G.C.A. Contributed reagents/materials/analysis tools: G.C.A. and K.R.M. Wrote the paper: G.E.G.K., G.E.I., C.H.C.W., K.R.M. and G.C.A.

Additional Information

Supplementary information accompanies this paper at <https://doi.org/10.1038/s41598-019-51193-x>.

Competing Interests: The authors declare no competing interests.

Publisher's note Springer Nature remains neutral with regard to jurisdictional claims in published maps and institutional affiliations.



Open Access This article is licensed under a Creative Commons Attribution 4.0 International License, which permits use, sharing, adaptation, distribution and reproduction in any medium or format, as long as you give appropriate credit to the original author(s) and the source, provide a link to the Creative Commons license, and indicate if changes were made. The images or other third party material in this article are included in the article's Creative Commons license, unless indicated otherwise in a credit line to the material. If material is not included in the article's Creative Commons license and your intended use is not permitted by statutory regulation or exceeds the permitted use, you will need to obtain permission directly from the copyright holder. To view a copy of this license, visit <http://creativecommons.org/licenses/by/4.0/>.

© The Author(s) 2019